Topologically Engineering of π-Conjugated Macrocycles: Tunable Emissions and Photochemical Reactions

Yi Liu,*[a,d]# Yang Feng,[a]# Peng Lei,[b]# Xindong Liu,[a] Xiaoqing Liu,[c] Siqi Zhang,[b] Bin Tu,[b] Chen Chen,[b] Qing-Dao Zeng*[b] and Lei Wang[a]

[a] Department Shenzhen Key Laboratory of Polymer Science and Technology, Guangdong Research Center for Interfacial Engineering of Functional Materials, College of Materials Science and Engineering, Shenzhen University, Shenzhen 518060, China. E-mail: liuyiacee@szu.edu.cn

[b] CAS Key Laboratory of Standardization and Measurement for Nanotechnology, CAS Center for Excellence in Nanoscience, National Center for Nanoscience and Technology (NCNST), Beijing 100190, China. E-mail: zengqd@nanoctr.cn

[c] Institute of Critical Materials for Integrated Circuits, Shenzhen Polytechnic, Shenzhen, 518055, China

[d] Centre for AIE Research, Shenzhen University, Shenzhen 518005, China

#These author contributed equally to this work.

Abstract: The topology of conjugated macrocycles had significant impacts on their photo-physical and photo-chemical properties. Herein, a series of π-conjugated macrocycles with diverse topology were synthesized via intramolecular McMurry coupling. Their chemical structure and macrocyclic topology were unambiguously confirmed via NMR, MALDI-TOF mass spectra, and scanning tunneling microscopy (STM). Depending on the structural topology and structural rigidity, these macrocyclic luminogens display obviously distinctive emission behavior and photochemical reactions in the solution and in the solid state. Monocyclic **MST** with lower strain was more susceptible to intramolecular motions, and thus exhibited aggregation-induced emission properties. After UV light irradiation, **MST** was also vulnerable to undergo photo-cyclization in solution and triplet sensitizer promoted photo-dimerization, and yielded the anti-dimer via triplet excimer on the HOPG surface confirmed by STM investigation. By contrast, highly constrained bis-macrocyclic luminogens **DMTPE**, featured with high emission quantum yields of 68% both in solution and in the solid state, was relatively inert to photochemical reactions and yield syn-dimer on the surface via singlet excimer involved [2+2] photo-dimerization.

Introduction

The exploration of structural diversities, complexities and topologies of molecules and frameworks was always the core task for chemists and material scientists.[1-2] Among them, π-conjugated macrocyclic molecules have attracted extensive attentions owing to their unique chemical structures and novel physical properties.[3-4] Compared with their acyclic counterparts, conjugated macrocycles were benefited with conformational rigidity and capability to form supramolecular complex in their inherent cavities. Tremendous efforts were devoted to the exploration of their diverse structures and topologies, such as the nanohoop like cycloparaphenylenes (CPPs),[5-9] zigzag hydrocarbon nanobelts,[10-11] spoked-wheel shaped dendritic polyphenylenes,[12-13] Mobius-strip shaped macrocycles.[14-15] Owing to their persistent structures and carbon-rich composition, the conjugated macrocycles have been regarded as the nano-sized substructures for diverse carbon allotropes and related materials,[16] like the relationship between CPP with carbon nanotube,[7] and dehydro[n]annulene with graphdiyne.[17-18] The adventure on the synthesis of these intriguing π-conjugated macrocycles not only shed clues on the fabrications of new carbon materials with diverse structures and dimensions, but also spurred the investigation on chemical and physical properties of complicated carbon structures based on these model compounds.

Parallel with the flourishing development of synthetic methods to access π-conjugated macrocycles, their applications in diverse fields had also emerged in the past decade.[3, 19-21] Originated from the infinite π-conjugated backbone, macrocycles had proven their unique electronic properties and performance in luminescent materials and organic electronics[20], ranging from emitters in organic light-emitting diodes[22-24], bio-imaging fluorophores[25] and sensors[26-29], to semiconductors in organic photodetectors[30], field effect transistor[31-32], and organic photovoltaic[33]. Beside their chemical composition, the topology of these conjugated macrocycles has determined their conformational geometry that they could explore and adopt, and thus controlled their electronic structure, self-assembling behavior, condensed structure and ultimate performance. However, the detailed topological influence on their photo-physical and photochemical properties was rarely explored, especially for the photochemical reactions between macrocycles.

In the past few decades, the phenylene vinylene macrocycles (PVMs), featured as structural

analogues of arylene ethynylene macrocycles, had been widely studied.[34-37] As the key component in PVMs backbone, stilbene was well known for its complicated and diverse photophysical and photochemical processes. Beside the radiative process like fluorescence and phosphorescence, stilbene could mainly undergo three types of photochemical reactions (Scheme 1): (i) fast unimolecular *cis-trans* isomerization; (ii) slow electrocyclic rearrangement of *cis*-S1 state to an isomeric 4a,4b-dihydrophenanthrene (**DHP**) and subsequent conversion to phenanthrene in presence of oxidants; (iii) very slow bimolecular [2+2] dimerization between an excited stilbene and a ground state stilbene to yield 1,2,3,4-tetraphenylcyclobutane (**TPCB**). Usually, these radiative and non-radiative processes of stilbene and related alkenes were competitive with each other, which were determined by their inherent chemical and electronic structures, as well as the exterior environments (like solvent polarity). For aryl-vinylene macrocycles with stilbene as key components, however, their photo-physical properties and photo-chemical process were still rarely explored, as well as the topological impacts on these photo-pumped processes.

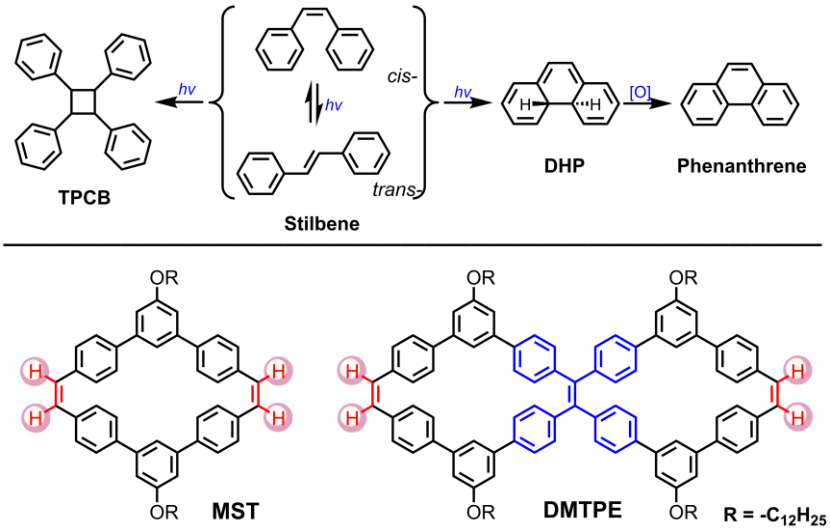

Scheme 1. Photochemical reactions related to stilbene and conjugated macrocyclic luminogens investigated in this work. (i) *cis-trans* isomerization; (ii) photocylization; (iii) [2+2] photodimerization.

Herein, we present the synthesis toward a series of π-conjugated PVMs luminogens with diverse topology (Scheme 1), whereas the macrocyclic topology was further confirmed via scanning tunneling microscopy (STM). The topology of the macrocyclic luminogens was revealed to be of great significance for their photophysical and photochemical properties. Compared with

monocyclic analogue **MST** which exhibited aggregation-induced emission behavior, bis-macrocyclic DMTPE was verified to be a dual-phase emitter.[38] The bis-macrocyclic backbone in DMTPE helped to restrict the intramolecular motions within the macrocycles, and thus turn on its emission in the solution via restriction of intramolecular motions (RIMs) mechanism. [39] On the other hand, the macrocyclic topology also plays a significant role in the photochemical process. In the solution, monocyclic **MST** could readily undergo photocyclization and triplet-sensitizer promoted photo-dimerization, and the bis-macrocyclic **DMTPE** was relatively inert to photochemical reactions. By contrast, both macrocycles underwent bimolecular [2+2] cycloaddition on the HOPG surface confirmed by STM, whereas **MST** yield the anti-dimer from its triplet excimer and DMTPE give out the syn-dimer from its singlet excimer.

Results and Discussion

As shown in the previous reports, PVMs were usually synthesized via reversible alkene metathesis, or irreversible McMurry and Witting reaction. Firstly, the synthesis toward bis-macrocyclic fluorophore **DMTPE** was attempted via ring closure olefin metathesis from alkene terminated precursor 1 with Grubbs 2nd generation catalyst in highly diluted condition (Scheme S1 in SI), in which the AIE-active tetraphenylethene (TPE) core could act as a template to facilitate the cyclization.[4] However, no targeted cyclic product was observed, whereas only oligomers had formed even after elongating the reaction time and raising the reaction temperature, indicated by the GPC curves of products (Table S1),. This was probably owing to the relative higher strain within the bis-macrocyclic product, which disfavored the yield of cyclic compound thermodynamically. Hence, the intramolecular McMurry coupling reaction[40-41] was applied to build-up the bis-macrocyclic luminogens **DMTPE** and monocyclic analogue **MST** from the aldehyde-incorporated precursor 2 and 3 (Scheme S1 and S2 in SI). Fortunately, the conjugated macrocycle **DMTPE** and **MST** were successfully obtained with a satisfactory yield of 38.8% and 24.7%, respectively. The template effect from the central TPE core was directly responsible for the higher yield of **DMTPE**, when compared with **MST**.

The chemical identities of these two macrocyclic compounds were unambiguously verified by ^{1}H nuclear magnetic resonance (NMR) spectroscopy and matrix-assisted laser ionization time-of-flight (MALDI-TOF) mass spectra (Figure 1). ^{1}H NMR spectra together with 2D

correlation spectroscopy (COSY) and nuclear Overhauser enhancement spectroscopy (NOESY) provided further structural proof for the macrocycles, where every proton signal could be unambiguously assigned (Figure 1a and 1c). The MALDI-TOF MS spectra of **DMTPE** and **MST** both indicated the presence of a single species with m/z = 1725.154 and 876.592, which were consistent with their desired molar mass. Additionally, the experimental isotopic distributions were also in perfect agreement with their simulated patterns (Figure 1b and 1d).

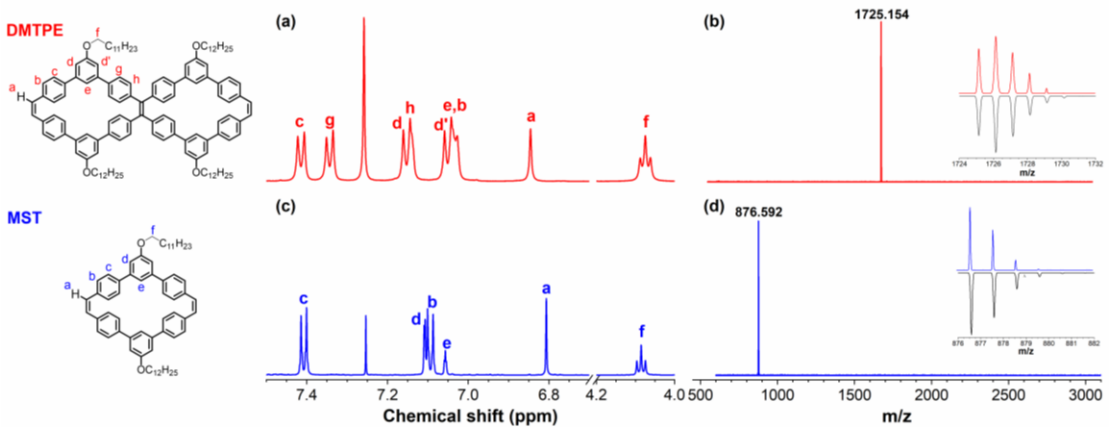

Figure 1. Partial ^{1}H NMR and MALDI-TOF MS spectra of π-conjugated macrocycles **DMTPE** (a and b) and **MST** (c and d).

In order to elucidate the cyclic topology of these macrocyclic compounds, their geometries were studied with density functional theory (DFT) calculations using functional B3LYP with the 6-31G(d) basis set. Their optimized structures clearly revealed the macrocyclic shaped topology and nano-porous backbone with highly twisted phenyl rings (Figure S3 in SI). For instance, the diameter of the void within the macrocyclic backbone in **DMTPE** and **MST** was approximately 0.4 nm. The homodesmotic calculations[42] of **DMTPE** and **MST** were also carried out to evaluate their strain energy within the rigid cyclic backbones (Figure S4 in SI). With their corresponding acyclic strain-released counterparts as comparison, **DMTPE** exhibited slightly raised strain within the bis-macrocyclic backbone when compared with its monocyclic analogue **MST**. And the strain energies of **DMTPE** and **MST** were calculated to be 14.6 kcal mol^{-1} and 12.7 kcal mol^{-1}, respectively.

To investigate the impacts of cyclic topology on the photo-physical properties of these macrocyclic luminogens, the UV–Vis absorption and photoluminescence (PL) spectra of these macrocycles were recorded in THF (Figure 2, Table S2). To better understand the significance of

cyclic skeleton, another derivative **TMTPE**, which was structurally featured with identical cyclic backbone of **DMTPE** and four peripheral free-rotating phenyl rings, was also synthesized and utilized as a comparison (Scheme S3). As recorded, their absorption spectra had gradually red-shifted following the order of **MST**, **DMTPE** and **TMTPE**, which was attributed to the π-conjugation extension from monocyclic to macrocyclic backbone and further attachment of phenyl rings. This result also agreed well with their simulated UV–Vis absorption spectra based on time-dependent DFT calculation using functional B3LYP with the 6-31G(d) basis set (Figure S5-S7). Furthermore, the molecular orbital and band gap of these macrocycles were also investigated via the theoretical calculations (Figure S8). Accordingly, their band gaps had decreased from 4.06 eV for monocyclic **MST**, to 3.63 eV for bis-macrocyclic **DMTPE**, and finally to 3.43 eV for **TMTPE**. As indicated, the HOMO and LUMO levels had both converged from monocyclic **MST** to bis-macrocyclic **DMTPE** skeleton. The introduction of peripheral phenyl rings only elevated the HOMO level from 5.13 eV for DMTPE to 4.92 eV for TMTPE, whereas these two bis-macrocyclic fluorophores share similar LUMO level.

Similarly, the emission spectra of bis-macrocyclic **DMTPE** in THF also exhibited a remarkable bathochromic shift from 462 nm for monocyclic MST to 502 nm, whereas **TMTPE** showed similar emission maximal at 506 nm. Additionally, the absolute emission quantum yield (Φ_{FL}) of these macrocycles was recorded to evaluate their photo-physical performance. The Φ_{FL} of macrocycles **MST** and **TMTPE** were determined to be 6.3% and 9.3% in their THF solution, 28.0% and 65.9% in the solid, respectively. This indicated that the monocyclic fluorophore **MST** and bis-macrocyclic luminogen **TMTPE** with free-rotating peripherals were evidently AIEgens. By contrast, bis-macrocyclic luminogen **DMTPE** without peripherals was proved to be a bright dual-phase emitter with high Φ_{FL} of 68.6% in the THF solution and 68.4% in solid.

Regarding their different emission capability in solution and solid, the PL spectra of these macrocyclic emitters in the solvent mixture of THF and water was further studied in detail. For **MST**, the emission enhancement in THF-H_2O mixture was as remarkable as observed in the solid, whereas its Φ_{FL} when f_w = 90% reached only 14.1% (Figure S9). This was probably owing to the molecular packing structure of **MST** in the aggregates, which had been found in the crystallization-induced emission phenomena. **DMTPE** was unveiled to be highly emissive in both the THF solution and as nano-aggregates (Figure S10). With raising water content (f_w) in the

THF-H_2O mixture, the PL spectra of **DMTPE** remained nearly identical when f_w < 10%. Afterward, the emission was slightly enhanced and gradually blue-shifted from 502 nm to 476 nm parallel with raising f_w (Figure 3a). The absolute fluorescence quantum yield of **DMTPE** in nano-aggregates (THF-H_2O mixture with f_w = 90%) was determined to be 86.7%. And the blue-shift of emission after aggregates formation was probably owing to the packing of fluorophroes in aggregates, which driven the fluorophore to adopt a more twisted conformation in the solid. As a result, bis-macrocyclic **DMTPE** was indeed a bright dual-phase emitter both in the solution and solid state, which overcame the dilemma of most organic fluorophores being either AIE-active or ACQ-active.[43-44] Featured with peripheral decoration, bis-macrocyclic **TMTPE** showed classical AIE behavior with enhanced and blue-shifted emission after addition of water (Figure S11), whereas its Φ_{FL} when f_w = 90% reached as high as 83.3%.

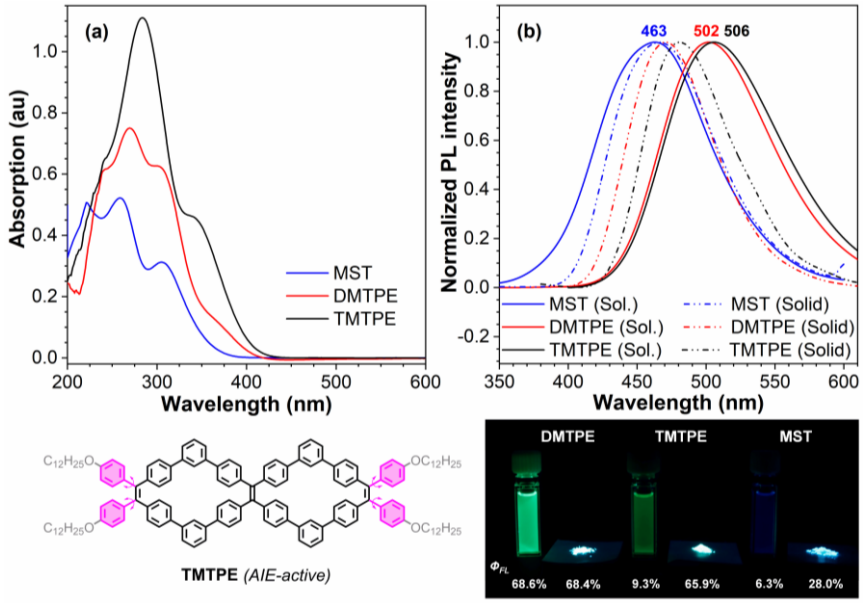

Figure 2. (a) UV-vis absorption spectra of π-conjugated macrocyclic fluorophores **DMTPE**, **MST** and **TMTPE** in the THF solution. (b) PL spectra of π-conjugated macrocyclic fluorophores in the THF solution and solid. Inset: chemical structure of AIE-active bis-macrocyclic analogues **TMTPE** and images (with emission quantum yield) of macrocyclic luminogens in the solution and solid under UV lamp. Concentration = 10 uM.

This sharp divergence in their emission brightness was probably attributed to the different cyclic topology, whereas these two macrocycles shared similar building blocks and strains. Although the *cis-trans* isomerization of stilbene moiety within these two macrocycles was prohibited, intramolecular motions (like rotation and vibration) were still possible for monocyclic

fluorophore **MST.** This finally resulted in the non-radiative decay of **MST** from its excited state and low emission efficiency in the solution, and these motions would be frozen in aggregate which facilitate the emission enhancement observed. For bis-macrocyclic analogue **DMTPE**, the bis-macrocyclic structure had significantly restricted the intramolecular motions of AIE-active TPE core in solution (including the rotation of phenyl rings or *cis-trans* isomerization of central alkene groups), and consequently led to the intense emission of **DMTPE** in THF.[45] In solid state, the highly twisted structure had diminished the intramolecular π-π interaction between **DMTPE**, similar to classical AIEgens. Therefore, intense emission was retained for **DMTPE** in the solid state by avoiding the detrimental stacking of normal ACQ fluorophores. In addition, the different conformations of **DMTPE** in THF solution and nano-aggregates were responsible for the changes of emission colors. When the macrocyclic luminogens were enforced to pack with each other in solid, the fluorophores were promoted to adapt more twisted conformations for densely packing. This would ultimately lead to the blue-shifted emission, which was commonly observed in the mechanochromic luminescence (MCL) of TPE-derived fluorophores.[26, 44, 46] After grinding and solvent annealing, the emission of **DMTPE** remained unchanged, whereas **TMTPE** exhibited obvious red-shifted emission after grinding and blue-shifted emission with solvent fuming (Figure S12). This distinction in the MCL behavior of **DMTPE** and its analogue **TMTPE** had further confirmed the shape-persistence and structural rigidity of **DMTPE**.

To further study the structures of the conjugated macrocycles, monolayers of these macrocycles luminogens on highly oriented pyrolytic graphite (HOPG) were investigated by STM at the liquid/solid interface (Figure 3). As shown in Figure 3a and 3b, the backbone of mono-cyclic **MST** appeared as a ring which was arranged head-to-tail closely and lined in arrays. The void of each mono-cyclic **MST** backbone is darker in the STM image. By contrast, the backbone of bis-macrocyclic **DMTPE** appeared as an 8-shaped dual-ring as shown in Figure 3d and 3e, and each dual-ring was arranged head-to-tail closely and lined in arrays. The middle portion of each **DMTPE** macrocycle backbone is brighter in the STM image, which corresponds to the central TPE moiety with higher electron density. Referring to the corresponding molecular models in Figure 3c and 3f, it can be seen that the ditches between the adjacent arrays are filled with the interlaced alkyl side chains of **DMTPE** and **MST**. The molecular arrangement is stabilized by the π-π interaction between the conjugated macrocycle and the HOPG substrate, and

the van der Waals force between the alkyl side chains. The unit cell parameters of each macrocycle were summarized in Table S6, whereas the total energy and energy per unit area for the self-assembled structures were also presented in Table S7.

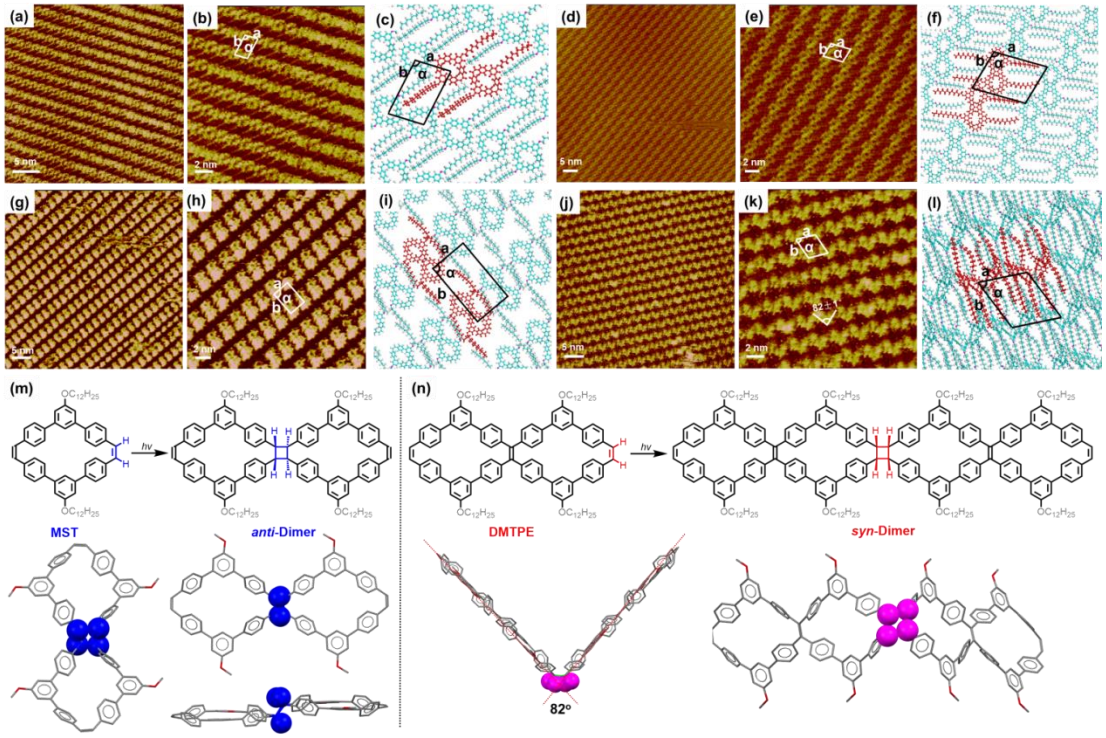

Figure 3. Self-assembled structures of macrocycles **MST** and **DMTPE** at the 1-phenyloctane -HOPG interface and their corresponding DFT calculated models. STM image (a), high-resolution STM image (b), and proposed molecular model (c) of **MST** self-assembly. Imaging parameters: I_{set} = 366.2 pA, V_{bis} = 742.8 mV. STM image (d), high-resolution STM image (e), and proposed molecular model (f) of DMTPE self-assembly. Imaging parameters: I_{set} = 381.5 pA, V_{bis} = 556.6 mV. STM image (g), high-resolution STM image (h), and proposed molecular model (i) of **MST** self-assembly after UV irradiation. Imaging parameters: I_{set} = 338.7 pA, V_{bis} = 661.3 mV. STM image (j), high-resolution STM image (k), and proposed molecular model (l) of **DMTPE** self-assembly after UV irradiation. Imaging parameters: I_{set} = 213.6 pA, V_{bis} = 856.3 mV. Photo-chemical [2+2] cycloaddition reaction and optimized geometry for the *anti* or *syn*-dimer of macrocyclic MST (m) and bis-macrocyclic **DMTPE** (n) observed in STM investigation, whereas the dodecyl chain was replaced with methyl group for clarity.

Considering the possibility of [2+2] photo-dimerization for stilbene, the self-assembled monolayer was further irradiated with UV light to explore the on-surface photochemistry of these macrocycles. Unexpectedly, the STM images of self-assembled structures for **MST** had obviously

transformed from the head-to-tail arrayed ring topology to shoulder-by-shoulder lined 8-shaped dual-ring array, whereas the experimental unit cell parameter had expanded from a = 1.4 ±0.1 nm; b = 2.3 ±0.1 nm, α = 100±1° to a = 2.0±0.1 nm, b = 3.4±0.1 nm, α = 90±1°. Assisted by the structure modeling, the newly observed species was probably owing to the anti-dimer of **MST** (as shown in Figure 3m) which originated from the dimerization alkene-terminated mono-cyclic MST via [2+2] photo-dimerization. By contrast, the dual-ring structure of **DMTPE** had evolved to lined "V"-shaped bright spots after UV light irradiation. The experimental unit cell parameter had transformed from a = 2.9±0.1 nm, b = 2.1±0.1 nm, α = 104±1° to a = 2.3±0.1 nm, b = 2.7±0.1 nm, α = 65±1°. According to the stereochemistry of [2+2] dimerization, this observed species was consistent with the syn-dimer of **DMTPE** from [2+2] cycloaddition of terminal double bond. The angle of "V"-shaped spot was determined to be 82o in the STM image, which was identical to the value determined from optimized geometry of the syn-dimer (Figure 3n). Furthermore, the experimental unit cell parameters for the UV-irradiated samples of the macrocycles **DMTPE** and **MST** agreed well with their theoretical models as shown in Figure 3i and 3l. Therefore, these two macrocycles could undergo stereo-selective [2+2] dimerization on the HOPG interface depending on the topology of the macrocycles. The geometry and energy of the *anti*- and *syn*-dimers for these two macrocycles were calculated, which indicated that the *anti*-dimers for both **MST and DMTPE** were thermodynamically more stable than their *syn*-dimers (Figure S13). Therefore, the stereo-selectivity observed via STM was probably attributed to the reaction mechanism rather than thermodynamic factors.

To reveal the photochemical mechanism of these macrocycles, the ^{1}H NMR of **DMTPE** and **MST** was investigated after UV light irradiation, in absence or presence of benzophenone (BP) as the triplet sensitizer. For mono-cyclic **MST**, the macrocycle was extremely ready to photochemical reaction, and the signal at 6.81ppm corresponding to the proton on terminal alkene moiety had completely disappeared after UV light irradiating. To evaluate the photochemical product, two characteristic peaks at 9.46 and 3.46 ppm were studied in detail. The former signal was attributed to the phenanthrene ring from photocyclization of stilbene, whereas the later was owing to the cyclobutane unit from [2+2] photo-dimerization. This was also confirmed via MALDI-TOF mass spectra of the irradiated samples (Figure S14). The mass spectra suggested a species with m/z of 873.03 after light irradiation, which was consistent with the molar mass of cyclized macrocycles

MST-4H. Additionally, a series of peaks had also been observed around m/z = 1760, which also suggested the formation of dimers after photo-irradiation.

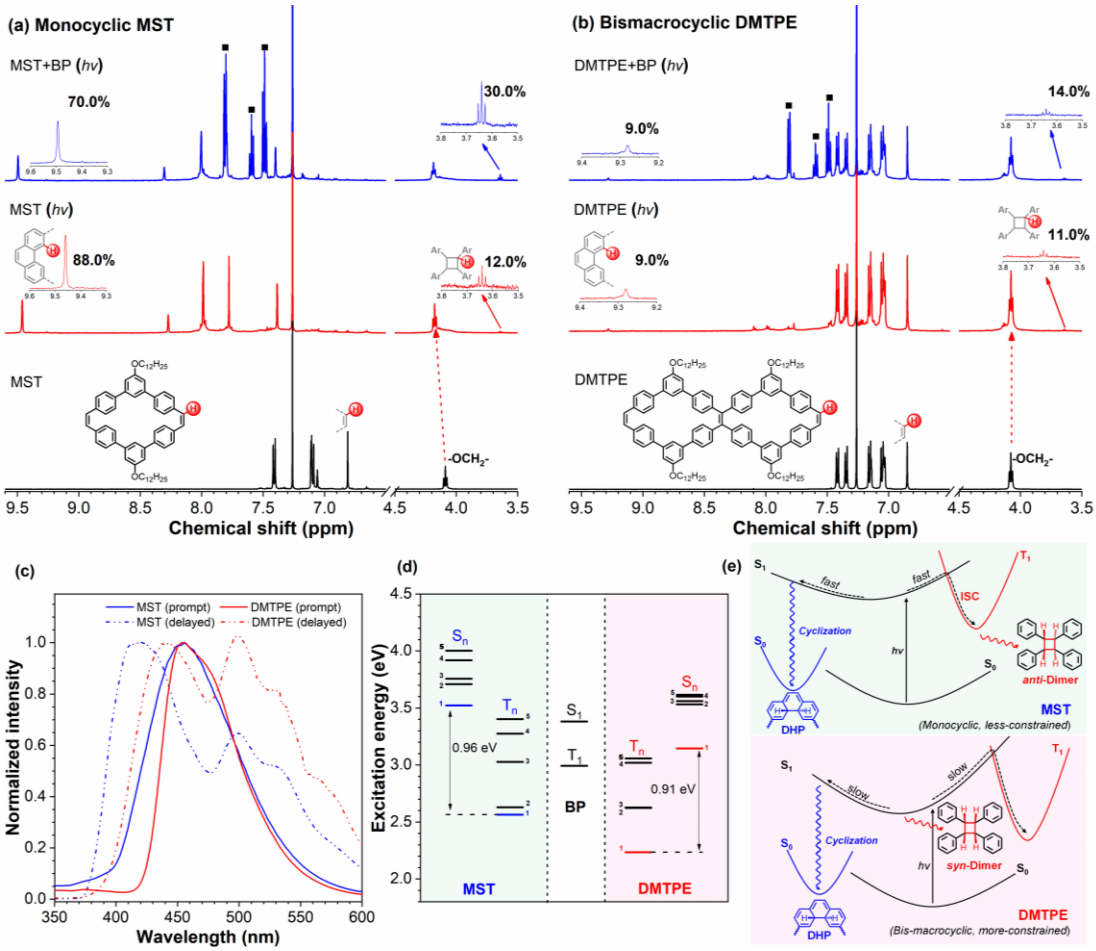

Figure 4. ^{1}H NMR spectra of macrocycles **MST** (a) and **DMTPE** (b) after UV light irradiation (hv) for 30 minutes in absence or presence of triplet sensitizer benzophenone (BP, ■) in $CDCl_3$. (c) PL spectra of macrocycles **MST** and **DMTPE** in toluene at 77K. (d) Energy diagrams of singlet (S_n) and triplet (T_n) excited states for triplet sensitizer BP, macrocycles **MST** and **DMTPE**. (e) Illustrative scheme for the photochemical reactions of macrocycles **DMTPE** and **MST**. S_0 and S_1 stand for the singlet ground state and the first singlet excited state, whereas T_1 is the triplet state.

According to the integral of these two peaks, the conversion of the macrocycles along these two photochemical approaches was estimated. Obviously, photo-cyclization was the dominating pathway for MST under UV light, whereas the high yield of photo-cyclized product was probably owing to the inherent cis-configuration of the stilbene moiety in the monocyclic skeleton. Only approximate 12% of the double bond in **MST** had been engaged in the [2+2] dimerization in

absence of BP. However, conversion toward the dimer product was obviously increased to 30% after addition of BP, whereas the yield of competitive photo-cyclized product decreases correspondingly. This trend clearly demonstrated that triplet excited state was probably involved in the [2+2] photo-dimerization of monocyclic MST. Furthermore, the casted film of **MST** was exposed to UV irradiation for 2 hours, surprisingly no cyclized product could be observed in the ^{1}H NMR spectrum whereas only small amount (approximate 7%) of stilbene moiety was involved in [2+2] photo-dimerization (Figure S15). This result clearly suggested the significance of structural motions in the photochemical reactions of conjugated macrocycles.

By contrast, the bis-macrocyclic **DMTPE** was quite inert to photochemical reactions, whereas only trace amount of the macrocycles had underwent the photo-driven cyclization and dimerization reactions. According to the integral at 9.28, 6.84 and 3.64 ppm, it was found that only about 9% of the terminal cis-stilbene unit in **DMTPE** had been photo-cyclized regardless of the existence of triplet sensitizer BP in the mixture. Meanwhile, the yield of cyclobutane from [2+2] dimerization was slightly promoted from 11% to 14% parallel after the addition of BP. The lower photo-chemical reactivity of **DMTPE** was probably attributed to the rigid skeleton in the bis-macrocyclic skeleton, which hampered the configuration transition requested in photochemical reaction. The small influence of triplet sensitizer on the conversion of cyclobutane moiety also indicated that the triplet excited state played a neglectable role in its photo-dimerization reactions of **DMTPE**. The solid sample of **DMTPE** was also irradiated, and no cyclized product could be observed in the ^{1}H NMR spectrum identical to the case for **MST** (Figure S15). However, obviously nearly 22% of stilbene moiety was converted to cyclobutane via [2+2] photo-dimerization. This remarkably raised yield compared with the investigation in the $CDCl_3$, was owing to the packing and close distance between adjacent macrocycles which was critical for the bimolecular [2+2] dimerization.

For cyclic alkenes (such as coumarin,[47-48] chromone,[49] and acenaphthylene[50-51]), their photochemical behavior had been widely studied. It was found that direct irradiation which only involved singlet excimer only yield the *syn*-dimer, whereas the triplet state which usually generate from the triplet sensitized reaction would give both *syn* and *anti*-dimers depending on the solvent. Therefore, the nature of the excited intermediate was probably responsible for the stereo-regularity observed in on-surface photo-dimerization for **DMTPE** and **MST**.

The singlet and triplet excited state for these macrocycles were studied via their prompt and delayed PL spectra measured in toluene at 77 K, as well as time-dependent density functional theory (TD-DFT) calculation for the mono-cyclic **MST** and bis-macrocyclic **DMTPE** using functional B3LYP with the 6-31G(d) basis set (Figure 4c and 4d). Both macrocycles displayed fluorescence around 450 nm and well-resolved delayed luminescence. The first delayed emission peak for both macrocycles was unexpectedly blue shifted relative to their prompt emission peak. This was probably attributed to that this phosphorescence signal was originated from the *m*-terphenyl segment[52] instead of the whole macrocycle. And thus the delayed emission from the entire macrocycles was attributed to the second delayed emission at 500 nm. The similar prompt and delayed emission for both macrocycles indicated that these two macrocycles had identical energy splitting (ΔE_{ST}[11]) between the lowest singlet (S_1) and triplet (T_1) excited states. This was also confirmed by the TD-DFT results, ΔE_{ST}[11] for **MST** and **DMTPE** was calculated to be 0.96 and 0.91 eV, respectively. Therefore, ΔE_{ST} was probably not the driving force toward the different tendency toward triplet state for **MST** and **DMTPE**. Usually, the intersystem crossing (ISC) from the excited singlet state to the triplet state was dependent on their energy splitting and structural reorganization. Therefore, monocyclic **MST** with lower reorganization energy was more ready to approach T_1 via ISC or sensitization reaction with BP, and the triplet state involved photo-dimerization of **MST** yield the *anti*-dimer on HOPG. By contrast, bis-macrocyclic **DMTPE** with highly constrained geometry and higher reorganization energy experienced the dimerization reaction via singlet excimer to form only *syn*-dimer on the surface.

For stilbene and related alkenes, their excited *cis*-S_1 states could also undergo an electrocyclic rearrangement to a DHP S_1 state, which would then relax to the DHP ground states and be converted to phenanthrene by mild oxidation. To approach the DHP state, structural rearrangement of *cis*-stilbene moiety was inevitably required. After UV light irradiation, a new absorption peak at 457 nm, which was attributed to the DHP intermediate, had appeared in the UV-Vis absorption spectra of MST (Figure S16). By contrast, the absorption spectra of **DMTPE** and **TMTPE** remained unchanged after irradiation. Therefore, the skeleton rigidity of the macrocycles would also be the dominating factor controlling their reactivity toward photo-cyclization (Figure 4e). Mono-cyclic **MST** with more relaxed structure and inherent *cis*-configuration for stilbene unit could smoothly rearrange to the DHP intermediate and

subsequently oxidized to phenanthrene. By contrast, highly constrained **DMTPE** skeleton was quite difficult to approach the DHP state via structural reorganization, and thus only 8% stilbene moiety was involved to form phenanthrene. This was also consistent with their photo-physical properties, whereas bis-macrocyclic **DMTPE** exhibited intense emission in solution due to restricted intramolecular motions and the emission efficiency for mono-cyclic **MST** was quite low owing to non-radiative intramolecular motions.

Conclusion

In summary, a series of π-conjugated macrocycles with different topology were successfully synthesized by intramolecular McMurry coupling. Their chemical identities and cyclic geometry were further confirmed via NMR, MALDI-TOF MS, and STM technique. Owing to different cyclic topology of the conjugated macrocycles, monocyclic **MST** showed low emission efficiency in the solution and AIE behavior in the solid state, whereas more constrained bis-macrocyclic **DMTPE** showed dual-phase emission behavior with high fluorescence quantum yield of 68% both in the solution and solid state. Additionally, these two macrocycles had shown distinctive photochemical behaviors on the HOPG surface and in solution. Monocyclic **MST** with less strained geometry was more ready for structural reorganization, and thus easier to approach the DHP intermediate and triplet state which yielded photo-cyclized product and *anti*-dimer. By contrast, highly constrained bis-macrocyclic **DMTPE** showed extremely low photochemical reactivity and produced the *syn*-dimer via singlet excited complex. These results had illustrated the significance of topology on the photo-physical and photo-chemical properties of conjugated macrocycles. The on-surface topology-dependent photo-dimerization between PVMs also opened up a new avenue for fabricating novel porous organic materials.

Acknowledgements

This work is partially supported by the National Natural Science Foundation of China (Nos. 21704065, 21773041, 21972031), National Key Basic Research Program of China (No. 2016YFA0200700), Guangdong Basic and Applied Basic Research Foundation (2021A1515010228), and the Innovation Research Foundation of Shenzhen (JCYJ20190808115215125). We thank the Instrumental Analysis Centre of Shenzhen University

(Xili Campus) for NMR measurement.

Keywords: Conjugated macrocycle • Topological engineering • Dual-phase emission • Photochemistry • Scanning tunneling microscope

Reference

[1] C. S. Diercks, O. M. Yaghi, *Science* **2017**, *355*, eaal1585.

[2] Z. Qiu, B. A. G. Hammer, K. Müllen, *Prog. Polym. Sci.* **2020**, *100*, 101179.

[3] M. Iyoda, J. Yamakawa, M. J. Rahman, *Angew. Chem. Int. Ed.* **2011**, *50*, 10522.

[4] Y. Jin, Q. Wang, P. Taynton, W. Zhang, *Acc. Chem. Res.* **2014**, *47*, 1575.

[5] M. R. Golder, R. Jasti, *Acc. Chem. Res.* **2015**, *48*, 557.

[6] S. Yamago, E. Kayahara, S. Hashimoto, in *Polycyclic Arenes and Heteroarenes* (Ed.: Q. Miao), Wiley-VCH, **2015**, pp. 143.

[7] H. Omachi, Y. Segawa, K. Itami, *Acc. Chem. Res.* **2012**, *45*, 1378.

[8] Z. Sun, T. Matsuno, H. Isobe, *Bull. Chem. Soc. Jpn.* **2018**, *91*, 907.

[9] M. Hermann, D. Wassy, B. Esser, *Angew. Chem. Int. Ed.* **2021**, *n/a*.

[10] T.-H. Shi, Q.-H. Guo, S. Tong, M.-X. Wang, *J. Am. Chem. Soc.* **2020**, *142*, 4576.

[11] T.-H. Shi, M.-X. Wang, *CCS Chem.* **2021**, *3*, 916.

[12] A. Idelson, C. Sterzenbach, S.-S. Jester, C. Tschierske, U. Baumeister, S. Höger, *J. Am. Chem. Soc.* **2017**, *139*, 4429.

[13] Y. Liu, A. Narita, J. Teyssandier, M. Wagner, S. De Feyter, X. Feng, K. Müllen, *J. Am. Chem. Soc.* **2016**, *138*, 15539.

[14] Y.-Y. Fan, D. Chen, Z.-A. Huang, J. Zhu, C.-H. Tung, L.-Z. Wu, H. Cong, *Nat. Commun.* **2018**, *9*, 3037.

[15] M. Stępień, L. Latos-Grażyński, N. Sprutta, P. Chwalisz, L. Szterenberg, *Angew. Chem. Int. Ed.* **2007**, *46*, 7869.

[16] F. Diederich, Y. Rubin, *Angew. Chem. Int. Ed.* **1992**, *31*, 1101.

[17] M. M. Haley, S. C. Brand, J. J. Pak, *Angew. Chem. Int. Ed.* **1997**, *36*, 836.

[18] W. B. Wan, S. C. Brand, J. J. Pak, M. M. Haley, *Chem. Eur. J.* **2000**, *6*, 2044.

[19] E. J. Leonhardt, R. Jasti, *Nat. Rev. Chem.* **2019**, *3*, 672.

[20] M. Ball, B. Zhang, Y. Zhong, B. Fowler, S. Xiao, F. Ng, M. Steigerwald, C. Nuckolls, *Acc. Chem. Res.* **2019**, *52*, 1068.

[21] Z. Qi, C. A. Schalley, *Acc. Chem. Res.* **2014**, *47*, 2222.

[22] S. Izumi, H. F. Higginbotham, A. Nyga, P. Stachelek, N. Tohnai, P. d. Silva, P. Data, Y. Takeda, S. Minakata, *J. Am. Chem. Soc.* **2020**, *142*, 1482.

[23] A. Yoshii, K. Ikemoto, T. Izumi, H. Taka, H. Kita, S. Sato, H. Isobe, *Org. Lett.* **2019**, *21*, 2759.

[24] J. Y. Xue, T. Izumi, A. Yoshii, K. Ikemoto, T. Koretsune, R. Akashi, R. Arita, H. Taka, H. Kita, S. Sato, H. Isobe, *Chem. Soc.* **2016**, *7*, 896.

[25] B. M. White, Y. Zhao, T. E. Kawashima, B. P. Branchaud, M. D. Pluth, R. Jasti, *ACS Cent. Sci.* **2018**, *4*, 1173.

[26] Y. Liu, F. X. Lin, Y. Feng, X. Liu, L. Wang, Z.-Q. Yu, B. Z. Tang, *ACS Appl. Mater. Interfaces* **2019**, *11*, 34232.

[27] X. Li, Z. Li, Y.-W. Yang, *Adv. Mater.* **2018**, *30*, 1800177.

[28] T. Naddo, Y. Che, W. Zhang, K. Balakrishnan, X. Yang, M. Yen, J. Zhao, J. S. Moore, L. Zang, *J. Am. Chem. Soc.* **2007**, *129*, 6978.

[29] J. Yu, C. Tang, X. Gu, X. Zheng, Z.-Q. Yu, Z. He, X.-G. Li, B. Z. Tang, *Chem. Commun.* **2020**, *56*, 3911.

[30] B. Zhang, M. T. Trinh, B. Fowler, M. Ball, Q. Xu, F. Ng, M. L. Steigerwald, X. Y. Zhu, C. Nuckolls, Y. Zhong, *J. Am. Chem. Soc.* **2016**, *138*, 16426.

[31] B. Zhang, R. Hernández Sánchez, Y. Zhong, M. Ball, M. W. Terban, D. Paley, S. J. L. Billinge, F. Ng, M. L. Steigerwald, C. Nuckolls, *Nat. Commun.* **2018**, *9*, 1957.

[32] W. Nakanishi, T. Yoshioka, H. Taka, J. Y. Xue, H. Kita, H. Isobe, *Angew. Chem. Int. Ed.* **2011**, *50*, 5323.

[33] S.-Q. Zhang, Z.-Y. Liu, W.-F. Fu, F. Liu, C.-M. Wang, C.-Q. Sheng, Y.-F. Wang, K. Deng, Q.-D. Zeng, L.-J. Shu, J.-H. Wan, H.-Z. Chen, T. P. Russell, *ACS Nano* **2017**, *11*, 11701.

[34] C. Liu, E. Park, Y. Jin, J. Liu, Y. Yu, W. Zhang, S. Lei, W. Hu, *Angewandte Chemie International Edition* **2018**, *57*, 8984.

[35] X. Hu, C. Yu, K. D. Okochi, Y. Jin, Z. Liu, W. Zhang, *Chem. Commun.* **2016**, *52*, 5848.

[36] C. Zhang, C. Yu, H. Long, R. J. Denman, Y. Jin, W. Zhang, *Chemistry – A European Journal* **2015**, *21*, 16935.

[37] Y. Jin, A. Zhang, Y. Huang, W. Zhang, *Chem. Commun.* **2010**, *46*, 8258.

[38] X. Zheng, W. Zhu, C. Zhang, Y. Zhang, C. Zhong, H. Li, G. Xie, X. Wang, C. Yang, *J. Am. Chem. Soc.* **2019**, *141*, 4704.

[39] Z. Zhao, H. Zhang, J. W. Y. Lam, B. Z. Tang, *Angew. Chem. Int. Ed.* **2020**, *59*, 9888.

[40] N. Delbosc, J. De Winter, S. Moins, A. Persoons, P. Dubois, O. Coulembier, *Macromolecules* **2017**, *50*, 1939.

[41] K. Nakao, M. Nishimura, T. Tamachi, Y. Kuwatani, H. Miyasaka, T. Nishinaga, M. Iyoda, *J. Am. Chem. Soc.* **2006**, *128*, 16740.

[42] C. E. Colwell, T. W. Price, T. Stauch, R. Jasti, *Chem. Sci.* **2020**, *11*, 3923.

[43] H. Wu, Z. Chen, W. Chi, A. K. Bindra, L. Gu, C. Qian, B. Wu, B. Yue, G. Liu, G. Yang, L. Zhu, Y. Zhao, *Angew. Chem. Int. Ed.* **2019**, *58*, 11419.

[44] S.-N. Lei, H. Xiao, Y. Zeng, C.-H. Tung, L.-Z. Wu, H. Cong, *Angew. Chem. Int. Ed.* **2020**, *59*, 10059.

[45] J.-B. Xiong, H.-T. Feng, J.-P. Sun, W.-Z. Xie, D. Yang, M. Liu, Y.-S. Zheng, *J. Am. Chem. Soc.* **2016**, *138*, 11469.

[46] Y. Q. Dong, J. W. Y. Lam, B. Z. Tang, *J. Phys. Chem. Lett.* **2015**, *6*, 3429.

[47] R. Hoffman, P. Wells, H. Morrison, *J. Org. Chem.* **1971**, *36*, 102.

[48] G. S. Hammond, C. A. Stout, A. A. Lamola, *J. Am. Chem. Soc.* **1964**, *86*, 3103.

[49] M. Sakamoto, M. Kanehiro, T. Mino, T. Fujita, *Chem. Commun.* **2009**, 2379.

[50] D. O. Cowan, R. L. E. Drisko, *J. Am. Chem. Soc.* **1970**, *92*, 6286.

[51] D. O. Cowan, R. L. E. Drisko, *J. Am. Chem. Soc.* **1970**, *92*, 6281.

[52] T. Fujii, S. Suzuki, H. Arita, *Chem. Phys. Lett.* **1984**, *111*, 350.

Entry for the Table of Contents

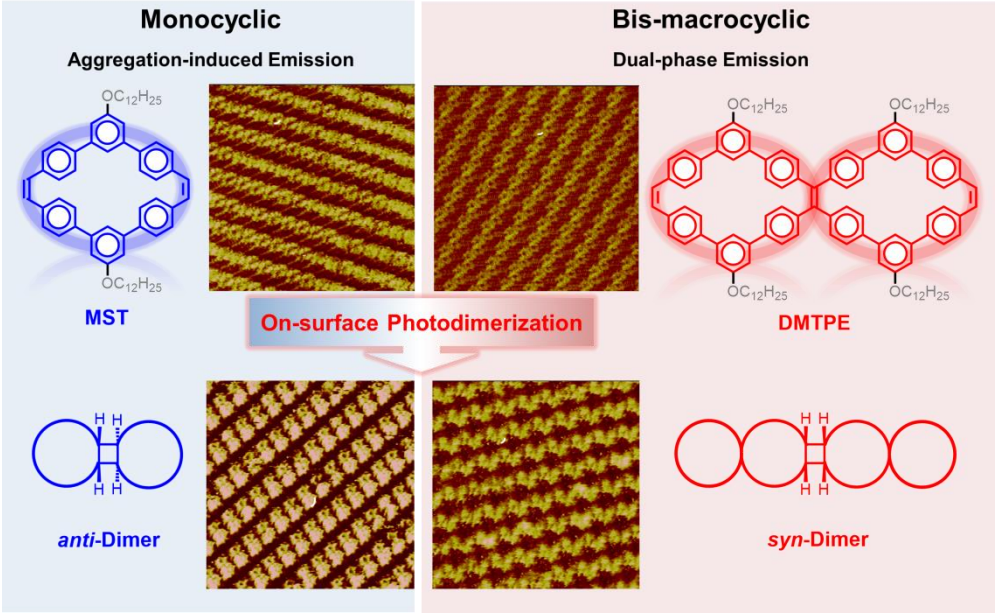

Topology of π-conjugated macrocyclic luminogens had dominated their photo-physical and photochemical process. Monocyclic lumonigen MST exhibiting AIE properties was converted to anti-dimer via triplet excimer on HOPG interface, whereas constrained bis-macrocyclic DMTPE featured with dual-phase emission experienced singlet excimer to yield syn-dimer on surface.